# Investigation of random lasers with resonant feedback

Y. Ling,[1] H. Cao,[1,*] A. L. Burin,[1,2] M. A. Ratner,[2] X. Liu,[3] and R. P. H. Chang[3]
[1]*Department of Physics and Astronomy, Materials Research Center, Northwestern University, Evanston, Illinois 60208-3112*
[2]*Department of Chemistry, Materials Research Center, Northwestern University, Evanston, Illinois 60208-3113*
[3]*Department of Materials Science and Engineering, Materials Research Center, Northwestern University, Evanston, Illinois 60208-3116*

(Received 2 October 2000; published 14 November 2001)

This paper presents a detailed experimental study of random lasers with resonant feedback. The dependences of the lasing threshold and the number of lasing modes on the transport mean free path, the pump area, and the sample size are measured. An analytical model based on the concept of quasistates is developed to explain the behaviors of random lasers.

DOI: 10.1103/PhysRevA.64.063808 PACS number(s): 42.55.Rz, 42.55.Ah, 42.25.Dd

## I. INTRODUCTION

Over the past few years, there have been several experimental [1–7] and theoretical [8–15] studies on random lasers. A random laser is different from a conventional laser in the feedback mechanism. A conventional laser consists of a gain medium and a cavity. The cavity, usually made of mirrors, provides coherent feedback for lasing. However, a random laser has no mirrors. The feedback is supplied by optical scattering in a disordered medium. Recently, random lasers with coherent feedback have been realized with highly disordered semiconductor powder and organic materials [5–7]. The performance of a random laser is determined by three characteristic length scales: the transport mean free path $l_t$, the gain length $l_g$, and the sample size $L$. In this paper, we present a quantitative experimental study of the dependence of the lasing threshold and the number of lasing modes on these length scales.

Several models have been set up in the theoretical study of stimulated emission in an active random medium, e.g., the diffusion equation with gain [8,10,11], the random walk and amplification of photons [12], and the ring laser with nonresonant feedback [13]. However, these models cannot predict lasing with coherent feedback because the phase of the optical field is neglected. A different approach has been taken recently, i.e., to directly calculate the electromagnetic field distribution in a random medium by solving the Maxwell equations using the finite-difference time-domain (FDTD) method [16,17]. The advantage of this approach is that one can model the real structure of a disordered medium and calculate both the emission spectrum and the spatial distribution of emission intensity at any time. However, the numerical simulation of three-dimensional random media with the FDTD method requires much computing power. Furthermore, the simulation must be done for thousands of samples with different configurations before any quantitative conclusion can be drawn. In the second half of this paper, we develop an analytical model for random lasers based on the concept of quasistates.

## II. EXPERIMENT

To study the effect of scattering strength on a random laser, we use polymer films containing laser dye and microparticles. The advantage of this system is that the gain medium and the scattering elements are separated. Thus, we can independently vary the amount of scattering by particle density and the optical gain by dye concentration.

Experimentally, Poly(methyl methacrylate) (PMMA) and rhodamine 640 perchlorate dye are mixed in dichromethane. Subsequently, titanium dioxide ($TiO_2$) microparticles are ultrasonically dispersed in the solution. The average size of the $TiO_2$ particles is 400 nm. Polymer sheets are made with the cell-casting technique. The film thickness is about 150 $\mu$m. The frequency-doubled output ($\lambda=532$ nm) of a mode-locked Nd:YAG (yttrium-aluminum garnet) laser (10 Hz repetition rate, 25 ps pulse width) is used as pump light. The pump beam is focused by a lens (6.3 cm focal length) onto the polymer sheet at normal incidence. The excitation spot on the film surface is about 50 $\mu$m in diameter. The emission from the polymer sheet is collected by a fiber bundle and directed to a 0.5-m spectrometer with a cooled charge-coupled device array detector.

We fabricate a series of polymer films with the same dye concentration but different particle density. The $TiO_2$ particle density in the polymer films varies from $8\times10^{10}$ to $6\times10^{12}$ cm$^{-3}$. The lasing threshold in these films is measured under identical conditions. Above the threshold, discrete narrow peaks emerge in the emission spectrum. The emission intensity there increases much more rapidly with the pump intensity. To characterize the transport mean free path in these films, we conduct coherent backscattering experiment [18,19]. The output from a He:Ne laser is used as the probe light, because of its wavelength being very close to the emission wavelength of rhodamine 640 perchlorate dye. To avoid absorption of the probe light, we fabricate PMMA films that contain only $TiO_2$ particles but not the dye. The thickness of the polymer films is about 400 $\mu$m, which is much longer than the transport mean free path in these films. From the angular width $w$ of the backscattering cone, we calculate the transport mean free path using the formula $l_t=\lambda/2\pi w(1+z_e)$, where $z_e$ is the extrapolated length ratio [20]. We assume that $z_e$ only depends on the overall reflectivity $R$ at the

*Email address: h-cao@northwestern.edu

 

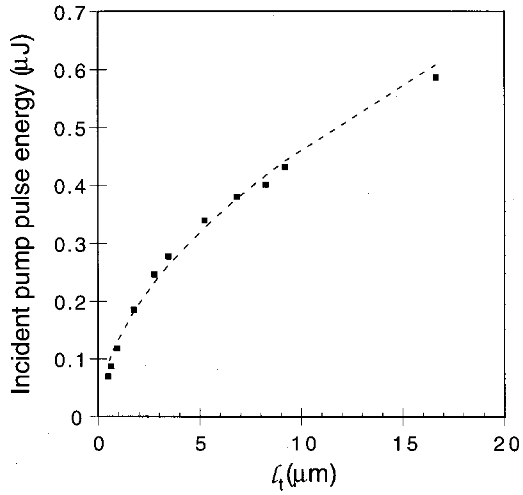


FIG. 1. Incident pump-pulse energy at the lasing threshold $P_{th}$ versus the transport mean free path $l_t$. The dashed line is the fitted curve represented by $P_{th}=0.13/l_t^{0.53}$.

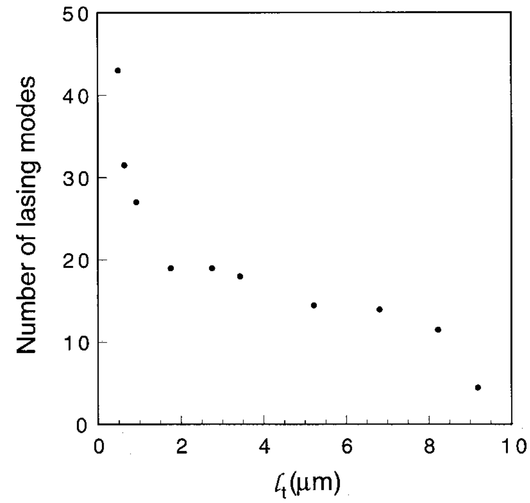


FIG. 2. Number of lasing modes as a function of the transport mean free path $l_t$. The incident pump-pulse energy is 1.0 $\mu$J.

film-air interface, i.e., $z_e=2(1+R)/3(1-R)$ [20]. For the PMMA films, we find $l_t$ is inversely proportional to the $TiO_2$ particle density $n_d$. More precisely, a curve fitting of $l_t$ versus $n_d$ gives $(1/l_t-1/l_0)\propto n_d$, where $l_0$ is the transport mean free path of the PMMA film without any $TiO_2$ particles. Note that recent studies show $z_e$ is determined not only by the overall reflectivity but also by the scattering anisotropy of individual particles [21]. Owing to the fact that the $TiO_2$ particles used in our experiment are strongly polydisperse, it is very difficult to calculate the anisotropy factor $g_s$ for the $TiO_2$ particles of different shape and size. If we assume all the $TiO_2$ particles are spherical and their diameter is equal to the average value 400 nm, we find $g_s\simeq 0.58$, and $z_e$ is reduced to 80% of its original value [21]. Correspondingly, the value of $l_t$ should be $\sim$20% larger than what we have estimated.

Figure 1 plots the incident pump pulse energy at the lasing threshold versus the transport mean free path. The dye concentration in the polymer film is fixed at $5\times10^{-2}$ M. As the $TiO_2$ particle density in the polymer film increases, the transport mean free path decreases, and the lasing threshold also decreases. The strong dependence of the lasing threshold on the transport mean free path clearly illustrates the important contribution of scattering to lasing. With an increase in the amount of optical scattering, the feedback provided by scattering becomes stronger. In other words, the laser cavities formed by recurrent light scattering have lower loss. Thus the lasing threshold is reduced. Through curvefitting, we find the lasing threshold is proportional to the square root of the transport mean free path. Figure 2 shows the number of lasing modes in the samples with different transport mean free path at the same pump intensity. The stronger the scattering is, the more lasing modes emerge. This is due to the fact that in a sample of stronger scattering strength, there are more low-loss cavities formed by the recurrent scattering. When the optical gain is fixed, the gain exceeds the loss in more cavities, and lasing oscillation occurs. An interesting feature in Figs. 1 and 2 is that when the transport mean free path approaches the optical wavelength, the lasing threshold pump intensity drops quickly, and the number of lasing modes increases dramatically.

One surprise from Fig. 1 is that lasing with resonant feedback occurs in samples where scattering is not very strong. For example, when the transport mean free path is 25 times the optical wavelength, lasing can still occur as long as the optical gain is high enough. To verify this, we fabricate polymer sheets with the same particle density but different dye concentration. Figure 3 plots the lasing threshold pump intensity versus the dye concentration. The $TiO_2$ particle density in the polymer films is fixed at $2.5\times10^{11}$ $cm^{-3}$. The relatively low particle density gives a rather long transport mean free path $l_t\sim$ 11 $\lambda$. From Fig. 3 the lasing threshold decreases with an increase of the dye concentration. When the dye concentration is below $4\times10^{-3}$ M, lasing could no longer occur at the maximum power of our pump laser. This result indicates that in a random laser the coherent feedback provided by the optical scattering is not necessarily very

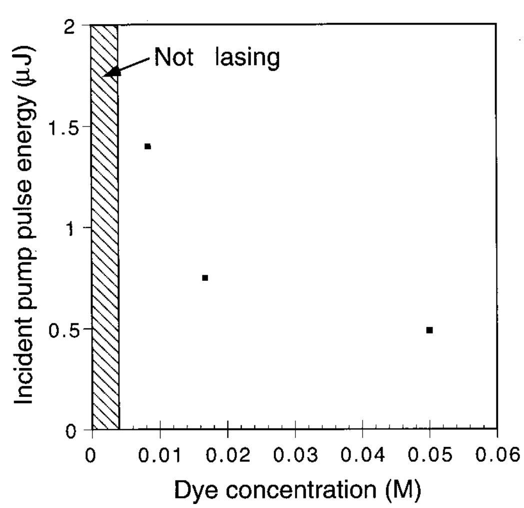


FIG. 3. Incident pump-pulse energy at the lasing threshold as a function of the dye concentration.

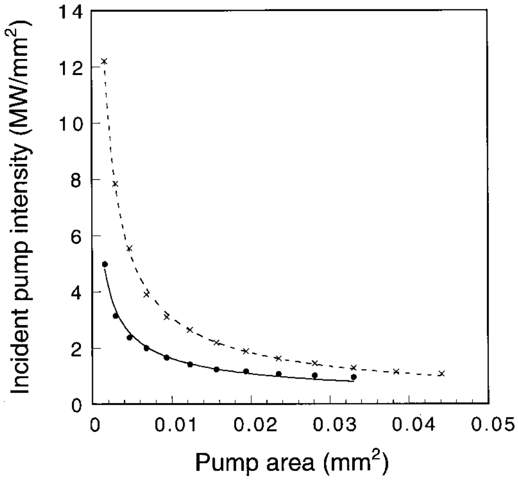


FIG. 4. Incident pump intensity at the lasing threshold $I_{th}$ versus the area $A$ of pump beam spot on the sample surface. The transport mean free path is 0.9 $\mu$m (circles), and 9 $\mu$m (crosses), respectively. The fitted curves are $I_{th}=0.11/A^{0.59}$ (solid line), and $I_{th}=0.096/A^{0.75}$ (dashed line).

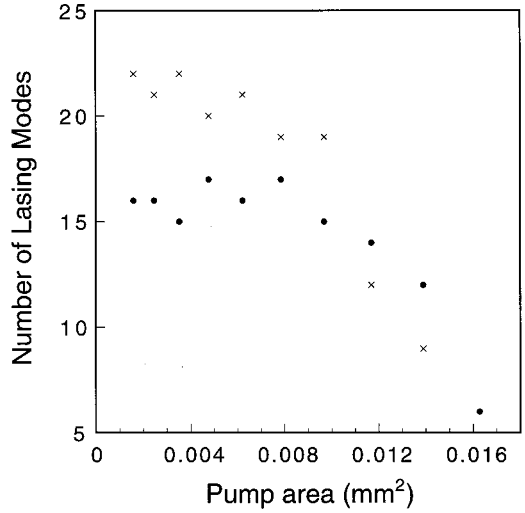


FIG. 5. Number of lasing modes versus the area of the pump beam spot on the sample surface. The transport mean free path is 0.9 $\mu$m (circles) and 9 $\mu$m (crosses), respectively. The incident pump pulse energies are 0.63 $\mu$J and 1.0 $\mu$J, respectively.

strong. In another word, the cavities formed by scattering can be lossy. As long as the dye concentration and the pump intensity are high enough, lasing with coherent feedback can occur.

The transport of light in a scattering medium depends not only on the transport mean free path, but also on the sample size. In an active random medium, the gain volume may be smaller than the medium volume, when only part of the disordered medium is excited. Next we study the dependence of a random laser on both the sample size (i.e., medium volume) and the gain volume. In particular, we will consider two cases. In the first case, the dimensions of the random medium are much larger than the transport mean free path, thus the medium can be considered infinitely large. But the gain volume is finite. In the second case, the random medium has a finite size and the entire medium is excited.

First, we vary the gain volume and measure the change of the lasing threshold. The PMMA film that contains dye and $TiO_2$ particles is initially placed at the focal plane of a lens. Then we move the lens away from the sample to increase the size of the pump beam spot on the sample. We measure the incident pump intensity at the lasing threshold $I_{th}$ as a function of the area of the pump spot on the film surface $A$. Figure 4 shows the data for two samples with different transport mean free paths. The circles (crosses) represent the data of the polymer film with higher (lower) $TiO_2$ particle density. The transport mean free path in these two samples is measured to be 0.9 $\mu$m and 9 $\mu$m, respectively. For both samples, the measured $I_{th}$ decreases as the pump area $A$ increases. Next we measure the number of lasing modes as a function of the pump area. In this measurement, we fix the incident pump power and vary the pump area. Thus, the incident pump intensity also changes with the pump area. Figure 5 plots the number of lasing modes versus the pump area for two samples with different transport mean free paths. The circles (crosses) correspond to the sample with the transport mean free path of 0.9 (9) $\mu$m, and the incident pump-pulse energy is 0.63 (1.0) $\mu$J. For both samples, we observe a plateau in the number of lasing modes. Under constant pump power, the number of lasing modes stays nearly constant when the diameter of the pump spot increases from 50 to 110 $\mu$m. Eventually, when the pump beam diameter is larger than 110 $\mu$m, the number of lasing modes starts decreasing, because the pump intensity approaches the lasing threshold.

In the above case, the emitted photons may diffuse out of the gain volume into the passive random medium. After multiple scattering events, they may return to the active random medium [4,13]. Therefore, the volume of the random medium which is involved in the lasing process, is larger than the pumped volume. Next we will study the case where the size of the random medium is finite and it is equal to the size of the excitation region. To control precisely the size of the random medium, we have utilized the microfabrication technique to make patterns on zinc oxide (ZnO) polycrystalline films.

The ZnO films are deposited on sapphire substrates by pulsed laser ablation. A detailed description of the growth procedure and the structural characterization of the films have been given elsewhere [22,23]. The film thickness is about 350 nm. The high-resolution transmission-electron-microscope images show that the films consist of many irregularly shaped grains of the size between 30 and 130 nm. Since the transport mean free path is close to the film thickness, light is scattered in the plane of the ZnO film [24]. The optical confinement in the direction perpendicular to the film is achieved through index guiding. Hence, the ZnO film can be approximated as two-dimensional (2D) random medium. Light leakage from the top and bottom interfaces of the film is regarded as loss. Under optical pumping, we have observed lasing with resonant feedback in the ZnO polycrystalline films [5].

We etch the ZnO films to make an array of disks whose diameters vary from 2 to 40 $\mu$m. The etchant is a water

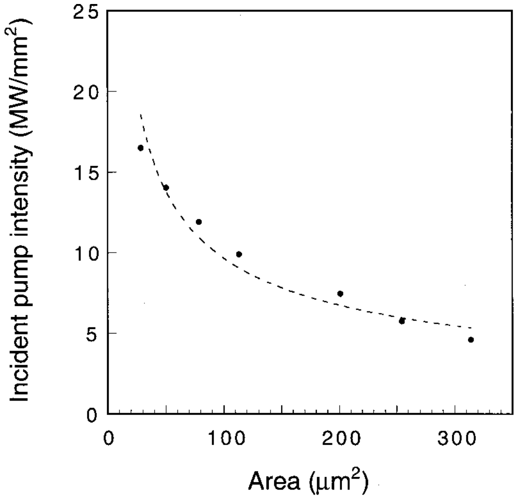


FIG. 6. Incident pump intensity at lasing threshold $I_{th}$ as a function of the ZnO disk area $A$. The dashed line is the fitted curve represented by $I_{th} = 104.5/A^{0.52}$.

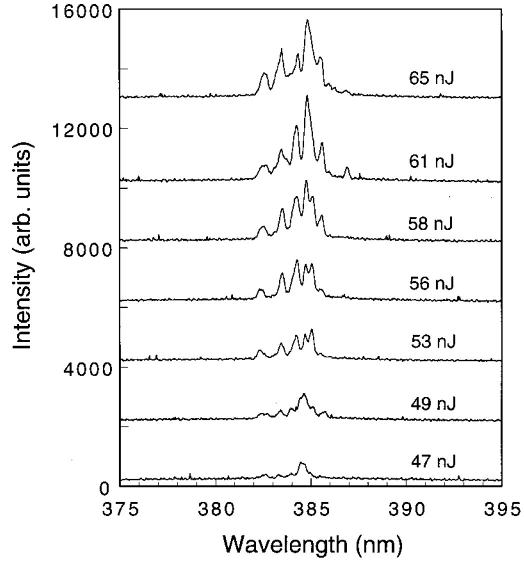


FIG. 7. Emission spectra from a ZnO disk of diameter 20 $\mu$m. The spectra are shifted vertically for clarity. The incident pump pulse energies are marked next to the curves.

solution of hydrochloric acid and hydrogen oxide. The scanning-electron-microscope images show that the edges of the disks are quite rough. Thus, the whispering-gallery modes could not be formed by total internal reflection at the disk edges. The patterned ZnO films are optically pumped by the frequency-tripled output of the mode-locked Nd:YAG laser. The pump beam is focused onto a single disk by a microscope objective lens. The pump beam spot covers the entire disk. Emission from the sample is collected by a fiber bundle and directed to the spectrometer.

Figure 6 shows the lasing threshold pump intensity $I_{th}$ versus the disk area $A$. The smaller the sample is, the higher the threshold pump intensity is. We curvefit the data in Fig. 6 with the formula $I_{th} \sim 1/A^x$, and obtain $x \simeq 0.52$. Since the disk diameter $d \sim \sqrt{A}$, we get $I_{th} \sim 1/d$, namely, the lasing threshold pump intensity is inversely proportional to the disk diameter.

The number of lasing modes is also sensitive to the sample size. Figure 7 plots the evolution of laser-emission spectra with the pump intensity for a disk of diameter 20 $\mu$m. Initially, the number of lasing peaks increases with the pump intensity. As the pump intensity increases further, the number of lasing modes does not increase any more, instead it saturates to a constant value. This value depends on the sample size. Figure 8 plots the saturated number of lasing modes versus the disk area. When the sample area is 30 $\mu\text{m}^2$, there are only three modes at high pump intensity. For the sample with an area of 320 $\mu\text{m}^2$, the number of the lasing peaks is saturated to seven. The saturation of the number of lasing modes has been predicted for the one-dimensional random structure [17]. Due to the gain competition, two random cavities with significant spatial overlap could not lase simultaneously. In other words, different lasing modes must be spatially separated. Hence, for a sample of finite size, only a limited number of lasing modes can exist even in the presence of high amplification. From Fig. 8, the saturated number of lasing modes increases with the sample area. From this data, we estimate the area that a single lasing mode occupies spatially is between 10 and 40 $\mu\text{m}^2$.

## III. MODEL

We start with the concept of quasistates for light in random media. The quasistates are the eigenmodes of the Maxwell equations in a finite-sized medium. The boundary conditions for quasistates are the absence of any incoming waves and the presence of only outgoing waves [25]. The frequency of a quasistate is a complex number, whose imaginary part describes the decay rate. Due to the complex values of the eigenenergies, the eigenmodes are not orthogonal to each other in the random medium. When photons in a quasistate reach the boundaries of the random medium, they are either reflected back to the medium or transmitted into the

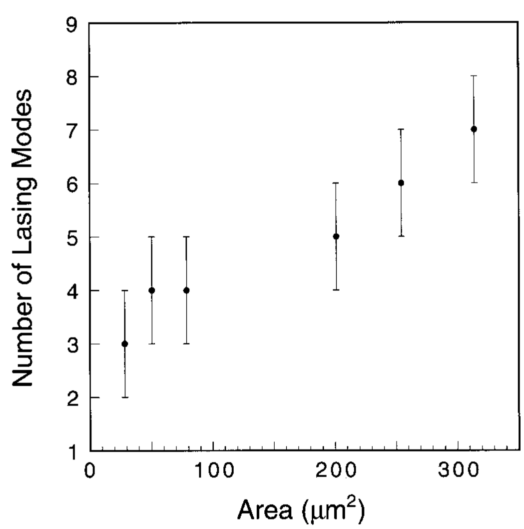


FIG. 8. Saturated value of the number of lasing modes as a function of the disk area. The error bar is also shown.

air. The transmitted photons are lost, while the reflected photons may get into other quasistates. Hence, the decay of a quasistate results from both light leakage through the boundaries and energy exchange with other quasistates. The mean decay rate $\gamma_d$ due to light leakage through the boundaries can be estimated as follows:

$$\gamma_d \sim \frac{D}{L^2}, \tag{1}$$

where $D$ is the diffusion coefficient and $L$ is the dimension of the random medium. The average frequency spacing between adjacent quasistates is

$$\delta\nu = \frac{v\lambda^2}{8\pi L^3}, \tag{2}$$

where $v$ is the speed of light in the medium. When $kl_t > 1$ ($k$ is wave vector, $l_t$ is the transport mean free path), $\gamma_d > \delta\nu$. Hence, the quasistates are spectrally overlapped, giving a continuous emission spectrum.

When the transport mean free path is much longer than the optical wavelength, the quasistates in a finite-sized random medium decay fast. Thus, their spectral lines are broad. The spectral overlap of the quasistates is significant. The quasistates are coupled strongly via reflection at the boundaries. Owing to the energy exchange among the quasistates, the loss of a set of interacting quasistates is much lower than the loss of a single quasistate. In an active random medium, when the optical gain for a set of interacting quasistates at the frequency of gain maximum reaches the loss of these coupled quasistates, the total photon number in these coupled states builds up. The drastic increase of photon number at the frequency of gain maximum results in a significant spectral narrowing. This process is called lasing with nonresonant (incoherent) feedback [8].

With an increase in the amount of optical scattering, the dwell time of light in the random medium increases, and the mixing of the quasistates is reduced because it occurs only at the boundaries. Hence, the decay rate of individual quasistates decreases. When the optical gain increases, it first reaches the threshold for lasing in a set of coupled quasistates. When the optical gain increases more, it exceeds the loss of a quasistate that has a long lifetime. Then, lasing occurs in a single quasistate. The spectral linewidth of the quasistate is reduced dramatically above this lasing threshold. A further increase of optical gain leads to lasing in more low-loss quasistates. Laser emission from these quasistates gives discrete peaks in the emission spectrum. This process is lasing with resonant (coherent) feedback [5–7].

When the scattering strength increases further, the decay rates of quasistates and the mixing among them continue decreasing. Due to the large dispersion of decay rates of quasistates, the threshold gain for lasing in individual low-loss quasistates becomes lower than the threshold gain for lasing in the coupled quasistates at the frequency of the gain maximum. Then, lasing with resonant feedback occurs first.

Therefore, there are two kinds of lasing processes in an active random medium, and they correspond to two lasing thresholds [26]. From the ray optics point of view, lasing with nonresonant feedback corresponds to the instability for light amplification along *open* trajectories in a random medium, while lasing with resonant feedback corresponds to the instability for light amplification along *closed* paths formed by recurrent scattering. Using quasistates, we can explain the behavior of the light transport in an active random medium from the diffusive regime to the localized regime. When $kl_t \gg 1$, the quasistate model predicts the same results as the diffusion model, as will be shown next. In the other extreme where $kl_t < 1$, the quasistate model approaches the random cavity model where the quasistates are the cavity modes [27].

Next, we first study lasing with nonresonant feedback using the quasistate model, and then move to lasing with resonant feedback. In the weak scattering regime, the loss of an individual quasistate comes from the loss of its photons to the surrounding air and to other quasistates. However, for a set of coupled quasistates, the total photon number $n_t$ is equal to the sum of the photon number in each quasistate. Hence, the exchange of photons among the quasistates is no longer a loss for the total photon number $n_t$. Namely, the decay for $n_t$ is caused solely by the light leakage through the boundaries. Its decay rate is expressed by Eq. (1), where $D = v l_t/3$. Under optical pumping, the gain rate for $n_t$ is $g = v/l_g$. When $g > \gamma_d$, $n_t$ increases with time. Hence, the threshold for lasing in a set of coupled quasistates is given by

$$g = \gamma_d, \tag{3}$$

which is the same as the threshold for lasing with nonresonant feedback given by the diffusion model [8].

For a polymer film containing dye and particles, the pump light hits the film surface and propagates inward. The gain volume can be approximated by a cylinder with diameter $d_p$ and height $l_p$, where $l_p$ is the penetration length of the pump light. In the linear absorption regime, the penetration length depends on the absorption length $l_a$ and the transport mean free path $l_t$. When $l_t < l_a$, $l_p$ is determined by the diffusion process of the pump photons inside the medium. The diffusion coefficient for the pump light is $D_p = v/(3/l_t + 1/l_a)$ [28]. Since $l_a > l_t$, $D_p \approx v l_t/3$. Thus, $l_p \approx \sqrt{l_t l_a/3}$ [4]. On the other hand, when $l_t > l_a$, the absorption is so strong that the pump light is absorbed before scattering occurs. Hence, $l_p \approx l_a$. In our experiments, the dye concentration and the $TiO_2$ particle density in the PMMA films are varied over a wide range. Our data cover both the diffusion regime ($l_a > l_t$) and the strong absorption regime ($l_a < l_t$). In the following theoretical analysis, we consider only the diffusion regime. A brief discussion of the strong absorption regime and the saturation of absorption will be given at the end of this section. Due to the lateral diffusion of the pump light, $d_p \simeq d + l_p$, where $d$ is the diameter of the incident pump beam spot on the sample surface [4]. Experimentally, $l_p$ is much shorter than $d$, thus $d_p \approx d$. When the optical transmission $T$ from the sample to the air is low enough, i.e., $T < l_t/l_p \approx \sqrt{3l_t/l_a}$, almost all the pump light passing through the air-sample interface is absorbed within the sample. The average density of the absorbed pump light is

$$I_p \sim \frac{I}{\sqrt{l_a l_t}}, \tag{4}$$

where $I$ is the input intensity of the pump light. Below we suppose that the gain rate, averaged over the excitation volume $g$, is proportional to the density of absorbed pump light $I_p$

$$g \propto \frac{I}{\sqrt{l_a l_t}}. \tag{5}$$

If the emission occurs due to electronic transition between some levels 2 and 1, and the population of lower level decays so fast that it can be neglected (e.g., due to multilevel dye structure suggested in Ref. [10]), then the gain rate would be proportional to the density of molecules $n_2$ having level 2 excited. In the regime of nonsaturated absorption $n_2$ is defined by the absorption rate leading to Eq. (5). From Eq. (3), the instability for $n_t$ occurs at the pump intensity

$$I_d \propto \sqrt{l_a l_t}\frac{l_t}{L^2}, \tag{6}$$

where $L$ should be the smallest dimension of the pumped cylinder. Since $d > l_p$, $L \sim l_p$ in Eq. (6). An accurate solution for the cylinder geometry of an active random medium gives the threshold gain rate [8]

$$g \propto \left( \frac{l_t}{l_p^2} + 10\frac{l_t}{d^2} \right). \tag{7}$$

We have generalized the above result to the geometry of our PMMA films and obtained the threshold pump intensity

$$I_d \propto \sqrt{l_a l_t}\left( \frac{l_t}{l_p^2} + 20\frac{l_t}{d^2} \right). \tag{8}$$

For our samples, $l_p$ is much shorter than $d$, thus the contribution of the second term in Eq. (8) is negligible. The lasing threshold is given by the first term, i.e.,

$$I_d \propto \sqrt{\frac{l_t}{l_a}}. \tag{9}$$

According to Eq. (9), the lasing threshold pump intensity is proportional to the square root of the transport mean free path $l_t$. If we assume $l_a \sim 1/n_{dye}$, the lasing threshold pump intensity is also proportional to the square root of the dye concentration $n_{dye}$. However, the lasing threshold should be independent of the pump beam diameter $d$ when $d > 20$ $\mu$m according to Eq. (8). This result is in contradiction to the data shown in Fig. 4. This is due to the threshold in Eq. (9) being for lasing in a set of coupled quasistates, while the measured threshold in Fig. 4 is for lasing in a single quasistate.

In fact, in the strong scattering regime where the photons of a quasistate are lost mainly to the surrounding air rather than to other quasistates, Eq. (9) also holds for the threshold of lasing in a single quasistate whose decay rate is equal to the average decay rate $\gamma_d$. However, the decay rates $\gamma$ of quasistates have a broad distribution. Hence, lasing could occur in some low-loss quasistates when the mean loss rate is still much larger than the gain rate [27]. In other words, the threshold for lasing in some low-loss quasistates can be much lower than the threshold $I_d$ in Eq. (9).

The statistical distribution of the decay rates of quasistates in a disordered medium depends on the transport mean free path and the sample size. Once the distribution function of decay rates $P(\gamma)$ is known, the distribution of lasing threshold, the mean value of lasing threshold, and the average number of lasing modes can be derived [27]. Next, we will derive the threshold for lasing in individual quasistates in the ZnO thin films and the PMMA films.

The ZnO film can be treated as a 2D random medium. For a ZnO disk of diameter $d$, the number of quasistates with frequencies within the full width of half maximum (FWHM) of the gain spectrum is

$$N \sim \frac{d^2}{\lambda^2}\frac{\Delta\lambda}{\lambda}, \tag{10}$$

where $\lambda$ is the center wavelength of the gain spectrum, $\Delta\lambda$ is the FWHM of the gain spectrum. For the PMMA films, we consider the quasistates that are located inside a cylinder of diameter $d$ and height $d$, and whose frequencies are within the FWHM of the gain spectrum $\Delta\lambda$. The total number of quasistates $N$ is

$$N \sim \frac{d^3}{\lambda^3}\frac{\Delta\lambda}{\lambda}. \tag{11}$$

Let $\gamma_\alpha$ and $g_\alpha$ be the decay rate and the gain rate for a quasistate $|\alpha\rangle$. The lasing occurs in $|\alpha\rangle$ when $\gamma_\alpha \leq g_\alpha$. We introduce the distribution function $f(y)$ for the ratio $y_\alpha = \gamma_\alpha / g_\alpha$. The mean value of $y$ is $y_0 \propto I_d/I$, where $I$ is the input pump intensity, and $I_d$ is the pump intensity needed to compensate the average loss of a quasistate. The probability distribution $f(y)$ can be expressed in the single parametric scaling form

$$f(y) = \frac{1}{y_0} h(y/y_0). \tag{12}$$

Since lasing occurs when $y \leq 1$, the probability for lasing in a quasistate at the pump intensity $I$ is

$$p_l = \int_0^1 \frac{dy}{y_0} h(y/y_0). \tag{13}$$

The average number of lasing modes $N_l = N p_l$, where $N$ is the total number of the quasistates. The lasing threshold is set by $N_l = 1$, namely, when there is one lasing mode.

The probability distribution $f(y)$ is determined by the fluctuation of the decay rates $\gamma$ and the gain rates $g$ of the quasistates. The gain rate $g$ depends on the spatial overlap of a quasistate with the pumped volume. For ZnO films, since the entire random medium is excited, the overlap is 100%. Moreover, because the optical gain is frequency dependent, quasistates of different frequencies experience different gain. However, since we consider only the quasistates within FWHM of the gain spectrum, the fluctuation of $g$ is small. On the other hand, for the PMMA films, the pumped volume and the quasistates may not completely overlap in space, resulting in a fluctuation of $g$. However, we believe the fluctuation of $g$ is less than the fluctuation of $\gamma$. Hence, we neglect the fluctuation of $g$ and attribute $f(y)$ to the fluctuation of $\gamma$. To obtain the distribution of $\gamma$, we use the results of the dynamics measurement reported by Genack *et al.* in Ref. [29]. When light passes through a random medium, the distribution of the delay time $\tau$ is taken as $P(\tau)\sim 1/\tau^3$, when $\tau$ is much longer than the average delay time $\tau_d$. This result has been explained theoretically from the assumption of the Gaussian distribution of the transmission through a chaotic medium by van Tiggelen *et al.* [30]. The transport of a photon through a random medium can be described as the capture of incoming photon by a quasistate and subsequent release to the environment. The decay rate of a quasistate $\gamma$ is related to the dwell time $\tau$ of light in the random medium, $\gamma = 1/\tau$. Accordingly, the distribution of the decay rates $P(\gamma)\propto\gamma$, when $\gamma \ll \gamma_d$. Neglecting the dispersion of the gain rate, we get

$$h(y)\propto y \tag{14}$$

when $y \ll y_0$. Due to the decay rate of some quasistates being much lower than the average decay rate $\gamma_d$, the threshold for lasing in such a quasistate $I_{th}$ is much less than $I_d$. Namely, $y_0 \gg 1$. Substituting Eq. (14) into Eq. (13), we get

$$N_l \sim \frac{d^m}{\lambda^m}\frac{1}{y_0^2}, \tag{15}$$

where $m$ is the dimensionality of the random medium. For the ZnO thin films $m=2$, while for the PMMA films $m=3$. From the lasing threshold condition $N_l \sim 1$, we find the dependence of the lasing threshold $I_{th}$ on various parameters. For the ZnO thin films, we get

$$I_{th}\propto \frac{1}{d}. \tag{16}$$

This result agrees with the data in Fig. 6, which give $I_{th} \propto A^{0.52} \propto 1/d^{1.04}$. For the PMMA films, we get

$$I_{th}\propto \frac{\sqrt{l_t}}{\sqrt{l_a}}\frac{1}{d^{3/2}}. \tag{17}$$

This means the threshold pump intensity is proportional to the square root of the transport mean free path, which is consistent with the data in Fig. 1. The dependence of lasing threshold on the pump area, given by Eq. (17), is $I_{th}\propto d^{-1.5} \propto A^{-0.75}$, where $A\sim d^2$. The data for the PMMA film with $l_t = 9\ \mu$m give $I_{th}\propto A^{-0.75}$, which is in excellent agreement with the theoretical result. However, for the PMMA film with $l_t = 0.9\ \mu$m, the data give $I_{th}\propto A^{-0.59}$. The discrepancy between the experimental result and the theoretical prediction may lie in the deviation of dwell time distribution from $P(\tau)\sim 1/\tau^3$ as $l_t$ approaches $\lambda$. Another possible source for the discrepancy is the transient optical gain. If we fit $I_{th}$ for the sample of $l_t = 0.9\ \mu$m with the formula $I_{th} = c_1 + c_2/A^{0.75}$, we obtain a very good fit with $c_1 = 0.47$ and $c_2 = 0.035$. This means Eq. (17) holds until $I_{th}$ is reduced to a saturated value $I_{sat} = 0.47$ MW/mm$^2$. The saturation of $I_{th}$ may result from the finite pumping time $\tau_p$. When the gain rate is below $g_{min}\sim 1/\tau_p$, lasing could no longer occur. Thus, $g_{min}$ sets the minimum pumping rate for lasing. Finally, in our calculation we neglect the fluctuation of the gain rates for quasistates. This simplification may also contribute to the discrepancy between the theoretical prediction and the experimental data.

Since the dependence of the lasing threshold on the sample size and the excitation area is obtained with the quasistate model, it holds for both regimes of $l_a < l_t$ and $l_a > l_t$. However, the square-root dependence of the lasing threshold on the transport mean free path is derived under the assumption $l_a > l_t$. When $l_a < l_t$, $l_p \approx l_a$ gives a linear dependence of the lasing threshold on $l_t$. Furthermore, the absorption of dye molecules can be saturated by strong pump light in some of our samples. In such cases, it can be shown that the lasing threshold $l_d$ is proportional to the square root of $l_t$, irrespective of the relative magnitudes of $l_a$ and $l_t$.

## IV. CONCLUSION

We have presented a detailed experimental study of the random lasers with coherent feedback. The lasing threshold pump intensity is proportional to the square root of the transport mean free path. The number of lasing modes also increases with a decrease of the transport mean free path. The strong dependence of the lasing threshold and the number of lasing modes on the transport mean free path confirms that the feedback for lasing is indeed provided by optical scattering.

The lasing threshold pump intensity also strongly depends on the pump area. For a 2D random medium, the lasing threshold pump intensity is inversely proportional to the square root of the sample area. The number of lasing modes first increases with the pump intensity, and eventually is saturated in a finite-sized sample. The saturation of the number of lasing modes results from the gain competition.

We have developed a model based on quasistates. This model can explain both the random lasers with nonresonant feedback and the random lasers with resonant feedback. Lasing with nonresonant feedback corresponds to lasing in a set of coupled quasistates, while lasing with resonant feedback corresponds to lasing in individual quasistates. Using the quasistate model, we have derived the dependence of the lasing threshold pump intensity on the transport mean free-path, the pump area, and the sample size. The theoretical predictions agree with the experimental results. However, to explain the behavior of random lasers well above the lasing threshold (e.g., to calculate the number of lasing modes), or to compare quantitatively with our data, more detailed theoretical study is required and many factors must be taken into account (e.g. the dynamics and saturation of the gain, the fluctuation of gain rate, etc).

## ACKNOWLEDGMENTS

We thank professor C. M. Soukoulis and Dr. X. Jiang for stimulating discussions. This work was supported in part by the National Science Foundation under Grant No. ECS-9877113. H. C. acknowledges financial support from the David and Lucile Packard Foundation and the A. P. Sloan Foundation. M.A.R. and A.L.B. thank the Chemistry Division of the NSF and the DoD/MURI program for support.

[1] N. M. Lawandy, R. M. Balachandran, A. S. L. Gomes, and E. Sauvain, Nature (London) **368**, 436 (1994).
[2] W. Sha, C.-H. Liu, and R. Alfano, J. Opt. Soc. Am. B **19**, 1922 (1994).
[3] C. Gouedard, D. Husson, C. Sauteret, F. Auzel, and A. Migus, J. Opt. Soc. Am. B **10**, 2358 (1993).
[4] G. van Soest, M. Tomita, and A. Lagendijk, Opt. Lett. **24**, 306 (1999).
[5] H. Cao, Y. G. Zhao, H. C. Ong, S. T. Ho, J. Y. Dai, J. Y. Wu, and R. P. H. Chang, Appl. Phys. Lett. **73**, 3656 (1998).
[6] H. Cao, Y. G. Zhao, S. T. Ho, E. W. Seelig, Q. H. Wang, and R. P. H. Chang, Phys. Rev. Lett. **82**, 2278 (1999).
[7] S. V. Frolov, Z. V. Vardeny, and K. Yoshino, Phys. Rev. B **57**, 9141 (1999).
[8] V. S. Letokhov, Sov. Phys. JETP **26**, 835 (1968) [Zh. Eksp. Teor. Fiz. **53**, 1442 (1967).
[9] Z.-Q. Zhang, Phys. Rev. B **52**, 7960 (1995).
[10] D. S. Wiersma and A. Lagendijk, Phys. Rev. E **54**, 4256 (1996).
[11] S. John and G. Pang, Phys. Rev. A **54**, 3642 (1996).
[12] G. A. Berger, M. Kempe, and A. Z. Genack, Phys. Rev. E **56**, 6118 (1997).
[13] R. M. Balachandran and N. M. Lawandy, Opt. Lett. **22**, 319 (1997).
[14] J. Herrmann and B. Wilhelmi, Appl. Phys. B: Lasers Opt. **B66**, 305 (1998).
[15] C. W. J. Beenakker, J. C. J. Paasschens, and P. W. Brouwer, Phys. Rev. Lett. **76**, 1368 (1999).
[16] H. Cao, J. Y. Xu, D. Z. Zhang, S.-H. Chang, S. T. Ho, E. W. Seelig, X. Liu, and R. P. H. Chang, Phys. Rev. Lett. **84**, 5584 (2000).
[17] X. Y. Jiang and C. M. Soukoulis, Phys. Rev. Lett. **85**, 70 (2000).
[18] M. P. van Albada and A. Lagendijk, Phys. Rev. Lett. **55**, 2692 (1985).
[19] P. E. Wolf and G. Maret, Phys. Rev. Lett. **55**, 2696 (1985).
[20] J. X. Zhu, D. J. Pine, and D. A. Weitz, Phys. Rev. A **44**, 3948 (1991).
[21] G. Popescu, C. Mujat, and A. Dogariu, Phys. Rev. E **61**, 4523 (2000).
[22] H. C. Ong and R. P. H. Chang, Phys. Rev. B **55**, 13 213 (1997).
[23] P. L. Washington, H. C. Ong, J. Y. Dai, and R. P. H. Chang, Appl. Phys. Lett. **72**, 3261 (1998).
[24] H. Cao, Y. G. Zhao, H. C. Ong, and R. P. H. Chang, Phys. Rev. B **59**, 15 107 (1999).
[25] L. D. Landau and E. M. Lifshitz, *Quantum Mechanics; Non-relativistic Theory* (Oxford, New York, 1977).
[26] H. Cao, J. Y. Xu, S.-H. Chang, and S. T. Ho, Phys. Rev. E **61**, 1985 (2000).
[27] T. Sh. Misirpashaev and C. W. Beenakker, Phys. Rev. A **57**, 2041 (1998).
[28] D. J. Durian, Opt. Lett. **23**, 1502 (1998); R. Aronson and N. Corngold, J. Opt. Soc. Am. A **16**, 1066 (1999); R. Graaff and J. J. Ten Bosch, Opt. Lett. **25**, 43 (2000).
[29] A. Z. Genack, P. Sebbah, M. Stoytchev, and B. A. van Tiggelen, Phys. Rev. Lett. **82**, 715 (1999).
[30] B. A. van Tiggelen, P. Sebbaa, M. Stoytchev, and A. Z. Genack, Phys. Rev. E **59**, 7166 (1999).